JTTEE5 15:717-724
DOI: 10.1361/105996306X146947
1059-9630/$19.00 © ASM International

Examination of Substrate Surface Melting-Induced Splashing During Splat Formation in Plasma Spraying

Chang-Jiu Li, Cheng-Xin Li, Guan-Jun Yang, and Yu-Yue Wang

(Submitted February 27, 2006; in revised form May 3, 2006)

Impacting of a molten droplet with a melting point much higher than the substrate results in melting of the substrate around the impact area. Melting of the substrate surface to a certain depth alters the flow direction of the droplet. The significant change of fluid flow direction leads to the detaching of fluid from the substrate. Consequently, splashing occurs during the droplet-spreading process. In the current study, molybdenum (Mo) splats were formed on a stainless steel substrate under different plasma-spraying conditions. For comparison, Mo splats were also deposited on an Mo surface. The substrate surface was polished prior to deposition. The powders used had a narrow particle size distribution. The results show that the morphology of splats depends significantly on the thermal interaction between the molten particle and the substrate. The splat observed was only a central part of an ideal disk-like complete splat. The typical pattern of Mo splats was of the split type, presenting a small split structure on the surface of the stainless steel substrate. With Mo particles, the preheating of a steel substrate has no effect on splat morphology. On the other hand, a disk-like Mo splat with a reduced diameter of a dimple-like structure at the central area of the splat was formed on Mo substrates, and splashing can be suppressed through substrate preheating. Based on the experimental results, a surface melting-induced splashing model was proposed to explain the formation mechanism of the Mo splat on a steel surface. The influence of droplet condition on splat formation is discussed.

Keywords droplet impact, molybdenum, plasma spray, splashing mechanism, splat formation

1. Introduction

A thermally sprayed coating is formed by a succession of molten droplets impacting on a substrate followed by lateral flattening, rapid solidification, and cooling. The behavior of a droplet after impacting on a substrate determines the interaction of the droplet with the substrate, the structure of the splat, and subsequently the adhesion of the coating to the substrate and the coating properties. Therefore, many investigations have been performed on splat formation in thermal spray processes. The advances in splat formation in plasma spraying have been summarized in two recent review studies (Ref 1, 2).

Based on substantial investigations, some fundamental phenomena have become clear. The splat formation process is influenced by the properties of both the droplet and substrate, and their interaction on impact. For example, the splashing occurs when the spray droplet impacts even on a flat substrate in ambient atmosphere (Ref 3). Moreover, splashing is suppressed when a flat substrate is preheated to a temperature over ~200 °C (Ref 4, 5). The suppression of splashing is essentially caused by the removal of evaporative substances adsorbed on the substrate surface through preheating (Ref 5, 6). However, our investigation suggested that when a molten droplet is deposited on a substrate with a much lower melting point than the droplet, the suppression of splashing through substrate preheating cannot be achieved (Ref 5). As a typical case, a molybdenum (Mo) splat deposited on a stainless steel surface presents a rather different morphology from other splat-substrate systems where both the droplet material and the substrate have similar melting points (Ref 7, 8). In this case, splashing occurs and cannot be suppressed by substrate preheating (Ref 5). Consequently, the splat presents a split morphology despite substrate preheating (Ref 5). It has been shown that Mo droplet impact causes the melting of a steel substrate (Ref 7-10). An Mo splat deposited on a steel surface presents a split, or so-called *flower-type*, splat (Ref 7, 8). And a metallurgical bonding between the resulting splat and the substrate forms (Ref 11). Our previous studies have pointed out that the formation of a split splat results from substrate surface melting on droplet impact (Ref 5, 8). This was confirmed recently by Zhang et al. (Ref 10) and Li et al. (Ref 12). Thereafter, Li et al. (Ref 12) proposed a temperature factor to determine the potential of substrate melting, which is related to the formation of the split splat. On the other hand, Mo splats deposited on a steel substrate presenting a nonsplit morphology can also be observed (Ref 8). This fact implies that the formation of split splats depends on the melting condition of the substrate surface, which is related to spray particle temperature. When substrate surface melting is localized to just a small area, the preheating of the substrate may suppress splashing, and consequently disc splats are observed on a preheated substrate (Ref 13-15). The purpose

This article was originally published in *Building on 100 Years of Success, Proceedings of the 2006 International Thermal Spray Conference* (Seattle, WA), May 15-18, 2006, B.R. Marple, M.M. Hyland, Y.-Ch. Lau, R.S. Lima, and J. Voyer, Ed., ASM International, Materials Park, OH, 2006.

Chang-Jiu Li, Cheng-Xin Li, Guan-Jun Yang, and **Yu-Yue Wang,** State Key Laboratory for Mechanical Behavior of Materials, School of Materials Science and Engineering, Xi'an Jiaotong University, Xi'an, Shaanxi, 710049 Peoples Republic of China. Contact e-mail: licj@mail.xjtu.edu.cn.

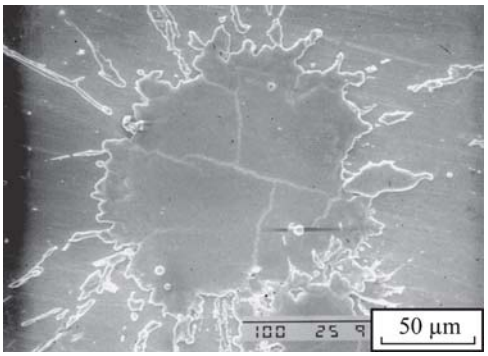

Fig. 1 Typical morphology of an Mo splat deposited on a stainless steel surface by a molten droplet generated at a plasma power of 30 kW

of the present article is to explain the formation mechanism of splats when droplet impact induces local substrate melting using molten Mo droplets created by different plasma conditions.

2. Materials and Experimental Procedures

Mo powders with two particle size ranges (76–90 μm and 45–53 μm) were used that were screened out from a commercial Mo powder (Metco 64). Stainless steel and Mo plates of 5 mm thickness were used as substrates. Before spraying, the surface of the substrate was polished with 1000-grit abrasive paper. To obtain isolated splats, a shielding plate with holes of 1 mm diameter was placed 50 mm in front of the substrate. Splats were formed by commercial plasma spray torches (model 9MB; Sulzer Metco, Winterthur, Switzerland; and GDP-80; Jiujiang, China). Both systems are in the 80 kW class of plasma-spraying equipment. Argon was used as a primary gas operated under a flow rate of 47 L/min at a supply pressure of 0.7 MPa, while hydrogen was used as a secondary gas at a supply pressure of 0.42 MPa. The flow rate of hydrogen gas was changed to change the plasma power through plasma arc voltage. The distance between the torch and the substrate was kept at 150 mm. During spraying, the powder feed condition was adjusted so that the spray particle stream passed through the plasma center to achieve effective heating and acceleration. With the GDP-80 system, an internal powder feeder port was used to achieve effective particle heating. Splat deposition was performed at different plasma powers. The morphology of sprayed splats was examined using scanning electron microscopy. The thickness profiles of typical splats were measured using a surface roughness tester (Kosaka Laboratory Ltd., Tokyo, Japan).

3. Experimental results

3.1 Effect of Spray Conditions on the Morphology of Plasma-Sprayed Mo Splats on Stainless Steel Surface

Figure 1 shows the morphology of a typical Mo splat sprayed at a plasma power of 30 kW on stainless steel. The radial arms surrounding the splat clearly indicate the occurrence of splashing during flattening. The diameter of the splat shown in Fig. 1 ranged from 120 to 150 μm. Taking into account the mean particle size of ~83 μm and a flattening ratio of 3 to 4 for molten droplets (Ref 16, 17), it is clear that this splat was only a central part of a complete splat (Ref 3, 18). The other parts of the splat surrounding this residual part have been splashed away. The flat surface of the splat indicates that it was deposited by a completely molten Mo droplet. Moreover, cracks were observed on the splat surface.

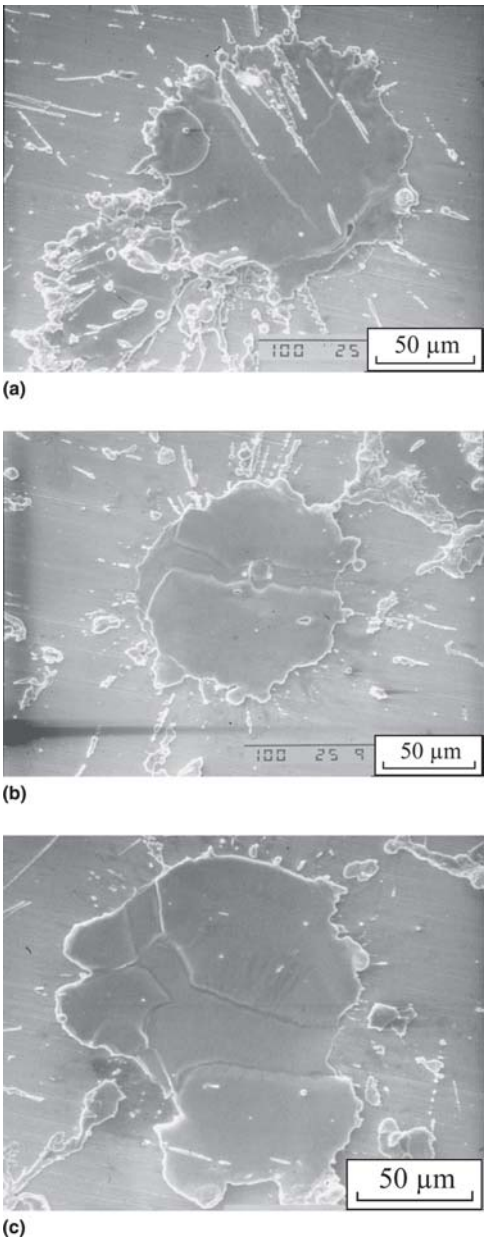

Fig. 2 Three Mo splats deposited on a stainless steel surface by molten droplets generated at a plasma power of 36 kW, representing different extents of splitting: (a) cracking; (b) limited splitting; and (c) remarkable splitting

Figure 2 shows the morphology of three typical splats sprayed under a plasma power of 36 kW. It can be observed that the splats shown in Fig. 2(a) and (b) have a diameter of ~100 μm.

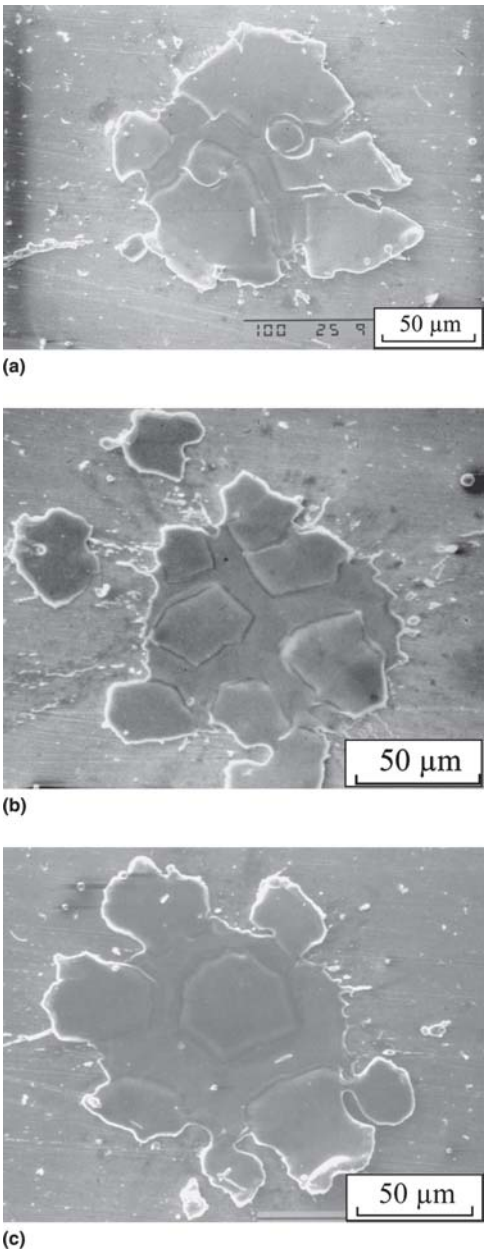

Fig. 3 Three Mo splats deposited on a stainless steel surface by molten droplets generated at a plasma power of 42 kW, representing remarkable splitting

Cracks were clearly observed on the splat shown in Fig. 2(a). The cracks that occurred on the surface of the splat shown in Fig. 2(b) are much wider than those shown in Fig. 2(a). In addition, the splat shown in Fig. 2(c) has split into three pieces. Evidently, those splats were only a fraction of a complete splat. Due to splashing, only a fraction of the central area of a complete splat was left on the substrate surface.

Figure 3 shows three typical Mo splats sprayed under a plasma power of 42 kW. All of those splats shown have a splitting morphology. Each splat was split into several small pieces. These splats have a size of ~100 μm. Evidently, these splats were also a fraction of a complete splat. Most of the splat material surrounding the residual part was splashed away. A detailed examination of the morphology of these splats indicates that small pieces were formed through the cracking of the central splat fraction after the surface was solidified. The measurement of the thickness profiles of the splat shown in Fig. 3(c) revealed that there appeared to be a crater surrounding the central split. Figure 4 shows an optical microphotograph of the splat shown in Fig. 3(c) and thickness profiles along three cross sections (A-A′, B-B′, and C-C′) of the splat. The split parts of the splat present a hill morphology. Moreover, it is clear from these profiles that the crater around the central split formed and had a depth of up to 2 μm.

3.2 Morphology of Mo Splat Deposited on Mo Surface

Figure 5 illustrates the morphology of an Mo splat formed on an Mo substrate under a plasma power of 42 kW. The detailed structure of the central area is shown in Fig. 5(b). The splat presents rather different splat morphology from those illustrated above for Mo splats on stainless steel. The examination into the detailed structure of such splats revealed that the splat presented a dimple-like structure in the central area that is similar to those observed in plasma-sprayed Cu and Ni splats on a stainless steel surface (Ref 3).

3.3 Effect of Preheating on Mo Splat Morphology

Figure 6 shows the typical morphology of Mo splats deposited on a stainless steel surface at a plasma power of 42 kW. The stainless steel surface was preheated to temperatures of 200 and 400 °C. These splats presented a similar split morphology as those deposited on the substrate surface in an ambient atmosphere without preheating.

Figure 7 shows the morphology of an Mo splat deposited on an Mo surface preheated to 200 °C. It is clear that a complete disk splat was formed under the preheating condition. The difference in morphology between the splats shown in Fig. 5 and Fig. 7 as a result of substrate preheating indicates that substrate materials influence the morphology of plasma-sprayed splats significantly.

4. Discussion

4.1 Surface Melting-Induced Splashing

The results obtained from this study clearly revealed that the morphology of Mo splats is influenced by plasma spray conditions, substrate materials, and substrate preheating conditions. For a completely molten Mo droplet, the subsequent splat sprayed onto a flat stainless steel surface results in a much smaller diameter than one would expect from splat thickness and droplet size. This fact indicates that much of the outer region of the splat has been splashed away during splatting, resulting in a smaller splat than is usually seen on a substrate surface.

The observation of Mo splats deposited on a stainless steel surface revealed that most splats have cracks distributed on the surface. It is possible that the cracking is caused by thermal shrinkage during the rapid cooling of the splat. A typical feature

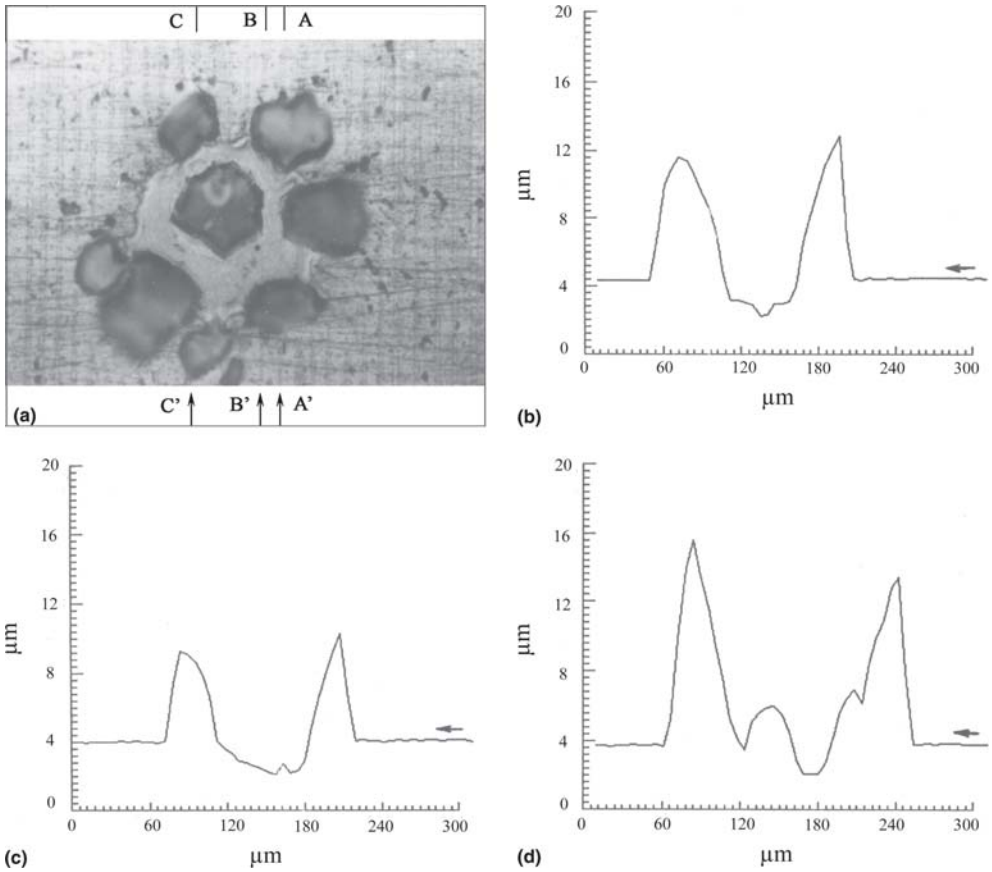

Fig. 4 Typical profiles across the Mo splat of Fig. 3(c) deposited on a stainless steel surface along the different positions shown in (a): (b) along the A-A′ line; (c) along the B-B′ line; and (d) along the C-C′ line

of Mo splats is that a central part of the splat is split into several small pieces. From the morphology of the splits and with use of imaging techniques, all of the splits can be reassembled to form a complete central part of the splat. Therefore, it is obvious that the splitting of the splat occurs after its coverage has been solidified. And the slipping of split pieces took place during the final stage of droplet flattening.

The detailed examination of the contact of the splits to the stainless steel substrate in the central area of the splat revealed a good contact without further cracking. For the stainless steel substrate, because its melting point is much lower than that of Mo, the melting of the substrate caused by the droplet during splatting is evident from the cross-sectional thickness profiles of the split splat. These results indicate that melted substrate material has flowed away to form the crater near the split. It was also clear that the preheating of the stainless steel substrate surface does not change the morphology of an Mo splat from a split type to a disk type. However, when Mo is used as a substrate, the morphology of the Mo splat is completely different. In an ambient atmosphere, the Mo splat presented a morphology similar to those observed for Cu, Ni splats deposited on stainless steel surfaces (Ref 3). When the substrate surface is preheated to a temperature of 200 °C, a complete disk splat is formed on the Mo surface. All the above results suggest that when an Mo splat is deposited on a stainless steel surface the flattening behavior is different from when an Mo splat is deposited on an Mo substrate, which has been reported previously (Ref 5, 6).

Based on the fact that the steel surface is melted on impact by the Mo droplet and the observed morphologies of Mo splats, the following surface melting-induced splashing mechanism is proposed. As shown in Fig. 8, when a molten Mo droplet impacts on a flat steel substrate, radial flow of the droplet fluid occurs along the substrate surface. At the same time, the rapid heat transfer to the substrate surface by the spreading droplet takes place. With the proceeding of droplet flattening, the substrate surface temperature rises continuously to cause local melting of the substrate surface. Due to a high dynamic pressure, the melted substrate material will be extruded to flow along the solid surface below the liquid Mo. This results in the formation of a crater around the impact point. The formation of the crater alters the fluid flow direction. As a result, droplet fluid tends to detach from the support of the substrate at the point where the crater intersects the substrate plane. When the dynamic pressure downward is not high enough to suppress the detachment of the fluid from the solid surface as the crater becomes large, the ejection of fluid occurs owing to the kinetic inertia of the flowing liquid. This leads to the ejecting of droplet material in the form of splashing. When splat deposition is performed at a preheating condition, the substrate temperature is raised and the substrate surface becomes more easily melted by the impacting Mo drop-

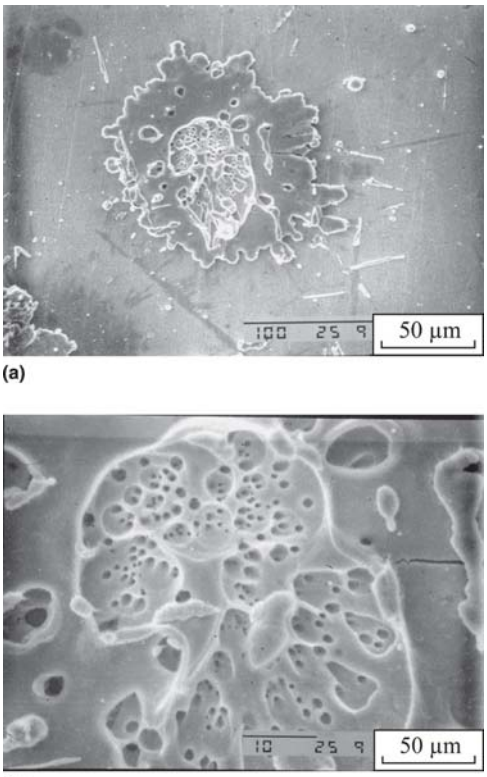

Fig. 5 (a) Morphology of typical plasma-sprayed Mo splats on an Mo surface in ambient atmosphere (b) with a detailed structure of the central area at a high magnification

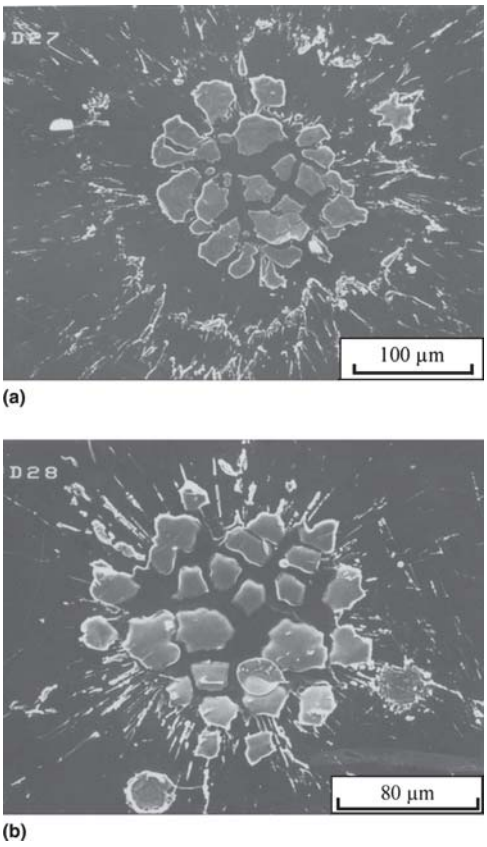

Fig. 6 Morphology of Mo splats deposited on the stainless steel surface preheated to temperatures of (a) 200 °C and (b) 400 °C

let. Consequently, a larger crater is produced, which promotes the splashing rather than the suppression of splashing, as has been observed for Ni, Cu splatting on a stainless steel surface (Ref 5, 6). This type of splashing can only be suppressed when the crater on the substrate surface induced by the molten droplet is so small that the change of fluid flow direction is not large enough to detach fluid from the substrate surface.

On the other hand, during the flattening process of the Mo droplet that has a much higher melting point than the substrate, solidification may start from the splat surface because the thermal radiation intensity from the molten Mo surface can be larger than the maximum heat transfer intensity by over three orders of magnitude, as discussed later. Due to the high melting point of Mo compared with that of stainless steel, a thin melted substrate layer may exist during the spreading of the Mo droplet. This layer covers the crater area under the splat. At the later stage of droplet flattening, solidification occurs in the area surrounding the crater. This leads to solidification of the melted substrate layer and welding of the droplet material to the substrate near the periphery of the crater. In this stage, thermal stress developed as the result of splat cooling. When such stress cannot be released through plastic deformation at low temperature, cracking of the central splat occurs. With a high-temperature Mo droplet sprayed at a high plasma power, a deeper crater is formed. Even though the cracking at the splat surface occurs, the splat fraction under solid coverage is possibly still in a liquid state. With

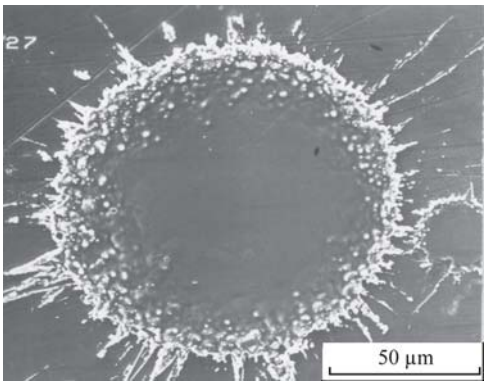

Fig. 7 Morphology of a typical Mo plasma-sprayed splat on an Mo surface preheated to 200 °C

further cooling, enough shrinkage force developed at the surface, which has been solidified, can pull the splat apart at the crack locations, resulting in splits floating on a film of thin liquid, as shown in Fig. 8(f). As a result, the Mo splat fraction surrounding the crater splits into several pieces. In addition, the slipping of the solidified split outward radially over liquid film causes splits surrounding central ones to push up (Fig. 8e) as suggested by Li et al. (Ref 12). This explains why the height of

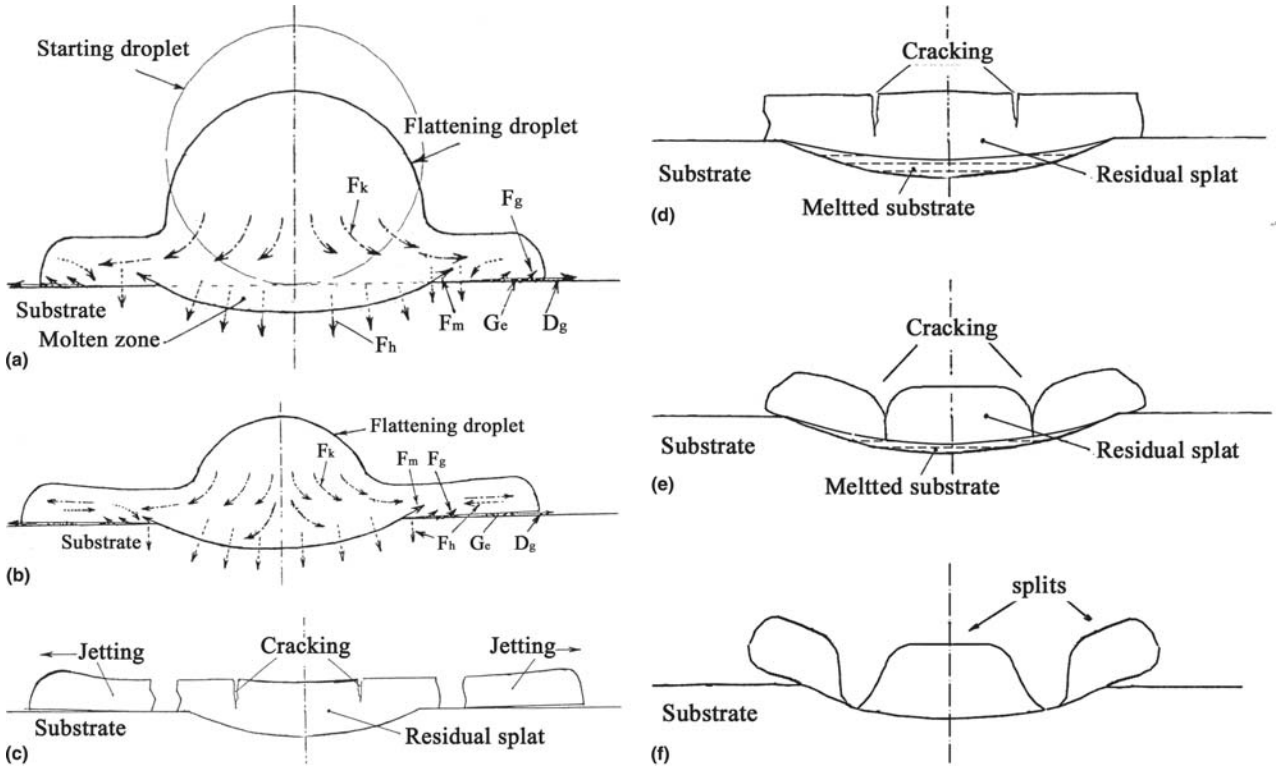

Fig. 8 Schematic diagram of droplet impact inducing the melting of a substrate and the flattening behavior of droplet resulting in the formation of a split-type splat. Fk indicates the flow direction of the spreading fluid driven by kinetic energy. Fh is the heat transfer direction from the droplet to the substrate. (a) and (b) indicate the early stages of flattening, resulting in the melting of the substrate by the impacting droplet. Fm indicates the flow direction of the spreading fluid resulting from the crater, which is formed by the melted substrate surface region. Fg indicates the direction of the evaporated gas-induced force. When flattening completes (c), the splashing occurs, driven by the inertial force of the rapidly flowing fluid along direction Fm. Cracking occurs as the surface layer of the splat is solidified, as shown in (c) and (d). The displacement by floating of the cracked splits on low-melting-point liquid film results in the formation of splitting of the residual central splat (e) and the final splat (f).

the split formed by a molten Mo droplet could reach >10 μm, as shown in Fig. 4.

For the case of a Ni droplet impacting on a Sn substrate, where the droplet has high plasticity and the substrate has a melting point much lower than that of the droplet, melting of the Sn substrate occurs, resulting in ejecting splashing, while splitting of Ni was not observed. Therefore, the ductility of the solidified splat and the surface tension of the liquid splat material are also factors that influence the splat morphology when the impacting droplet induces local substrate melting.

4.2 Influence of Limited Melting on Splat Formation

The temperature and heat capacity of a droplet determine the degree of substrate melting. A high-temperature Mo droplet obtained at a high plasma power promotes substrate melting and the formation of a completely split splat. On the other hand, a low-temperature Mo droplet causes limited substrate melting, which tends to suppress the slipping of the cracked splits. As a result, no splitting occurs, and only cracks are observed on the splat surface. The previous simulation investigation showed that the effective transient dynamic pressure of flattening a droplet on the substrate acts on the area where the flattening ratio is less than ~1.5 (Ref 19). In the case where the area of the crater on a substrate surface caused by an impacting droplet is less than this area on which the effective dynamic pressure has acted, the flow direction of droplet fluid cannot be significantly changed. Therefore, it would also be possible in the case of a small Mo droplet that the preheating of the substrate surface would promote the transient of particle morphology from an irregular splat to a regular disc splat (Ref 13). It can be considered that the disk Mo splats observed recently on preheated glass substrates (Ref 14, 15) are also an example of this case. Due to the much lower thermal conductivity of the glass, it can be considered that the melted local glass surface caused by the impact of an Mo droplet would be so shallow that it could not significantly alter the flow direction of the droplet spreading. As a result, an Mo droplet flattens to a disk splat on the preheated glass surface. The flattening degree of about 4 observed for such splats (Ref 15) is comparable to those of Cu splats (Ref 17). Therefore, in this case the spreading of the droplet is controlled by the viscous flow of the droplet fluid. The effect of surface tension on droplet flattening can be neglected. This result evidently indicates that the photographic technique developed by Moreau et al. (Ref 14, 15) for taking split-second images of a flattening Mo droplet is reliable. However, the image of an Mo splat that is deposited on the same glass at ambient temperature, yielding a much higher degree of flattening (up to 10) has not been well explained.

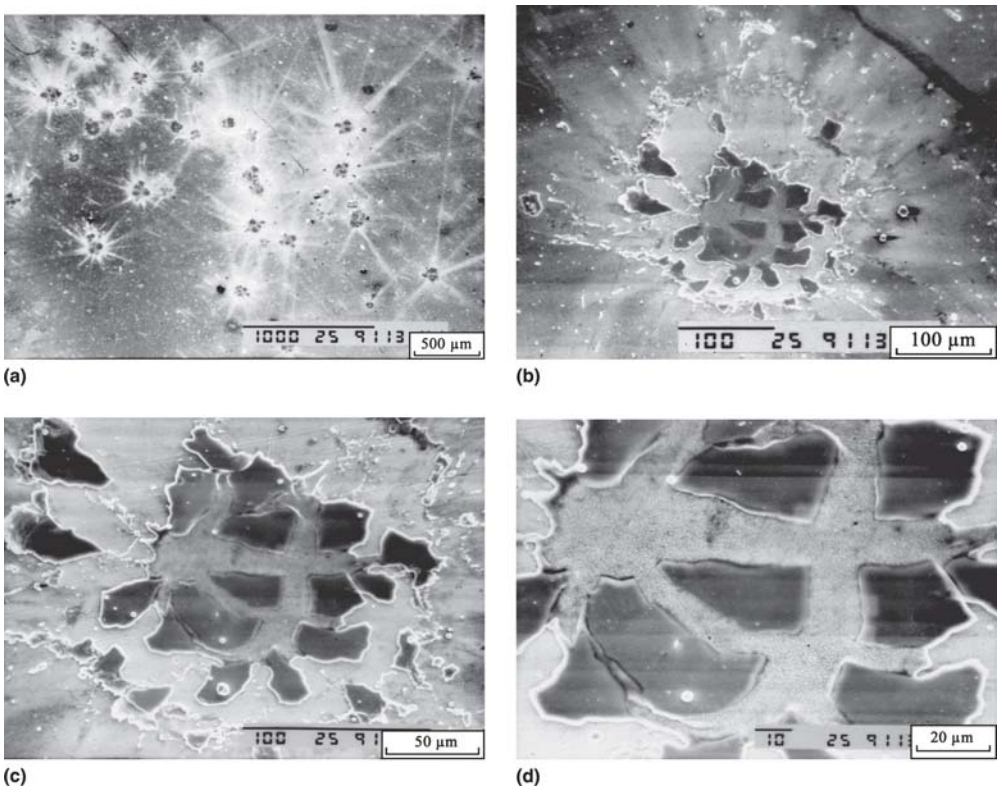

Fig. 9 An Mo splat deposited on a stainless steel surface at a plasma power of 42 kW in different magnifications. (a) General view of the splats; (b) splat with radial tracks representing jetting of the parted splat; (c) central part surrounded with splits; and (d) central split splat

Figure 9 shows images of Mo splats deposited at a plasma power of 42 kW at different magnifications. The center area presents the same split splat as that shown in Fig. 3. Moreover, several pieces of a parted splat attached to the substrate surface around the central area can be seen (Fig. 9 b, c). Possibly, this is due to the low inertia of those splits after parting from the central splat. Moreover, radial bright contrast on the substrate can be clearly observed in Fig. 9(a) and (b). This contrast resulted from the removal of the adsorbed organic reagent that was used for cleaning the substrate surface by the rapid heating of the spreading droplet. This indicates that this droplet kept contact with the substrate at the early stage of flattening, owing to the limited substrate surface melting. The evaporation of the evaporative adsorbates on the substrate resulting from the heating of the spreading droplet by heat conduction and radiation evolves a gas cushion between the substrate and the spreading liquid, as was suggested in our previous reports (Ref 5, 6). When a gas cushion is involved, the radial flow of the spreading liquid driven by the kinetic inertia and energy expense resulting from viscous flow may be neglected. The spreading should be dominated by the expense of kinetic energy to surface energy. The numerical simulations suggest that the initial flattening velocity of radial flow is about three times that of the droplet impact velocity (Ref 19). With the Mo splat deposited on the glass surface at room temperature reported by McDonald et al. (Ref 15), the average radial flow velocity of the flow front can reach ~300 m/s [to a radius of 240 μm in 0.8 μs (Ref 15)], which is over two times the initial droplet velocity of 135 m/s. This fact suggests a very rapid deceleration of the fluid front at the later flattening stage. On the other hand, even at a flattening degree of about 10, a simple estimation shows that the influence of surface tension on spreading is still limited. Therefore, the droplet would have flattened to a much larger size if only the surface tension effect was taken into account.

For a molten Mo droplet, a high surface temperature ~3000 K leads to a high radiation intensity of about 40×10^9 W/cm^2 following the Stefan-Boltzmann law of radiation (Ref 20). On the other hand, even for very low thermal contact resistance [10^{-7}–10^{-8} K m^2 W^{-1} (Ref 21)] the maximum heat flux at the splat-substrate interface for a temperature difference of 3000 K is 10^6 to 10^7 W/cm^2. Therefore, the magnitude of the maximum heat transfer intensity across the splat-substrate interface is less than the thermal radiation intensity by three orders or magnitude. As a result, the relatively strong radiation from the splat surface possibly causes the onset of surface freezing earlier by orders in magnitude compared with the solidification resulting from the interface heat transfer. Moreover, the intensive radiation between the splat under the surface and the glass may cause the rapid evaporation of adsorbates and the heating up of the gas, which results in a stable gas cushion. Therefore, it can be considered that flattening of the droplet liquid over a gas cushion to a thin liquid film will be continued until the local surface freezing begins and flattening inertia causes the parting of the splat, resulting in splashing. Although experimental evidence is necessary to confirm this speculation, the evident rupture of the splat in the solid state, as shown in Fig. 9, suggests the occurrence of solidification of the Mo splat from the surface and fracture of the splat in the solid state.

5. Conclusions

Mo splats deposited on the stainless steel surface formed by the molten droplets generated by plasma jet were only the central part of a complete splat. All other splat material surrounding this central part was splashed away. This type of splashing resulted from a localized melting of the substrate surface that was caused by the impacting droplet. The melted crater on the substrate surface alters the flow direction of the droplet fluid and tends to form a free liquid jet that detaches from the substrate surface. This type of splashing cannot be suppressed through substrate preheating. The results indicated that the flattening of a spray droplet is significantly influenced by localized melting of the substrate by the droplet on impact.

Cracking occurred to the Mo splat that was deposited on the steel substrate. This was due to the restraining of the splat contraction during cooling and to the low plasticity of the solidified splat material. The local welding of the splat to the substrate near the periphery of the molten crate increases the restraint of the splat contraction. A liquid film rich in the steel substrate material between the Mo splat and the substrate promoted the floating of Mo splits initiated from cracks. The high surface tension of liquid Mo promotes the formation of a split that is >10 μm high. A surface melting-induced splashing model is proposed, and it explains well the splashing involved in substrate melting. On the other hand, when an Mo splat is deposited on an Mo substrate with no substrate surface melting, the flattening process is influenced by surface adsorbates, as reported in a previous study (Ref 6). When substrate surface melting by the impact of a droplet is not deep enough to cause the spreading liquid to detach from contact with the substrate surface, the splashing is dominated by surface adsorbates.

References

1. P. Fauchais, M. Fukumoto, A. Vardelle, and M. Vardelle, Knowledge Concerning Splat Formation: An Invited Review, *J Thermal Spray Technol.,* 2004, **13,** p 337-360
2. H. Li, S. Costil, H.-L. Liao, C.-J. Li, M. Planche, and C. Coddet, Effect of Surface Conditions on the Flattening Behavior of Plasma-Sprayed Cu Splat, *Surf. Coat. Technol.,* 2006, **200,** p 5435-5446
3. C.-J. Li, J.-L. Li, W.-B. Wang, A. Ohmori, and K. Tani, Effect of Particle Substrate Materials Combinations on Morphology of Plasma Sprayed Splats, *Thermal Spraying: Meeting the Challenges of the 21st Century,* C. Coddet, Ed., May 25–29, 1998 (Nice, France), ASM International, 1998, p 481-488
4. M. Fukumoto, S. Katoh, and I. Okane, Splat Behavior of Plasma Sprayed Particles on Flat Substrate Surface, *Thermal Spraying: Current Status and Future Trends,* A. Ohmori, Ed., May 22–26, 1995 (Kobe, Japan), High Temperature Society of Japan, 1995, p 353-358
5. C.-J. Li, J.-L. Li, and W.-B. Wang, The Effect of Substrate Preheating and Surface Organic Covering on Splat Formation, *Thermal Spraying: Meeting the Challenges of the 21st Century,* C. Coddet, Ed., May 25–29, 1998 (Nice, France), ASM International, 1998, p 473-480
6. C.-J. Li and J.-L. Li, Evaporated-Gas-Induced Splashing Model for Splat Formation During Plasma Spraying, *Surf. Coat. Technol.,* 2004, **184,** p 13-23
7. J.M. Houben, Future Development in Thermal Spraying, *Proceedings of 2nd National Conference on Thermal Spray* (Long Beach, CA), American Society for Metal, 1984, p 1-18
8. C.-J. Li, A. Ohmori, and K. Tani, The Morphology of Plasma-Sprayed Molybdenum Splats, *Surface Modification Technology,* Vol X, T.S. Sudarshan, K.A. Khor, and W. Reitz, Ed., The Institute of Materials, London, 1997, p 934-945.
9. S. Sampath, X. Jiang, A. Kulkarni, J. Matejicek, D.L. Gilmore, and R.A. Neiser, Development of Process Maps for Plasma Spray: Case Study for Molybdenum, *Mater. Sci. Eng., A,* 2003, **348,** p 54-66
10. H. Zhang, X.Y. Wang, L.L. Zheng, and X.Y. Jiang, Studies of Splat Morphology and Rapid Solidification During Thermal Spraying, *Int. J. Heat Mass Transfer,* 2001, **44**(24), p 4579-4592
11. J.M. Houben and G.G.V. Liempd, Metallurgical Interactions of Mo and Steel During Plasma Spraying, *Proceedings of 10th International Thermal Spray Conference,* May 4-7, 1983 (Essen, Germany), German Welding Institute, 1983, p 66-71
12. L. Li, X.X. Wang, G. Wei, A. Vaidya, H. Zhang, and S. Sampath, Substrate Melting During Thermal Spray Splat Quenching, *Thin Solid Films,* 2004, **468,** p 113-119
13. H. Zhang, X.X. Wang, L.L. Zheng, and X.X. Jiang, Studies of Splat Morphology and Rapid Solidification During Thermal Spraying, *Int. J. Heat Mass Transfer,* 2001, **44,** p 4579-4592
14. N.Z. Mehdizadeh, M. Lamontagne, C. Moreau, S. Chandra, and J. Mostaghimi, Photographing Impact of Molten Molybdenum Particles in a Plasma Spray, *J. Thermal Spray Technol.,* 2005, **14**(3), p 354-361
15. A.G. McDonald, M. Lamontagne, C. Moreau, and S. Chandra, Visualization of Impact of Plasma-Sprayed Molybdenum Particles on Hot and Cold Glass Substrates, *Proceedings of the International Thermal Spray Conference (ITSC)* E. Lugscheider, Ed., May 2-5, 2005 (Basel Switzerland), ASM International, p 1192-1197
16. M. Vardelle, A. Vardelle, P. Fauchais, and C. Moreau, Pyrometer System for Monitoring the Particle Impact on a Substrate During a Plasma Spray Process, *Meas. Sci. Technol.,* 1994, **5,** p 204-212
17. C.-J. Li, H.-L. Liao, P. Gougeon, G. Montavon, and C. Coddet, Experimental Determination of the Relationship Between Flattening Degree and Reynolds Number for Spray Molten Droplets, *Surf. Coat. Technol.,* 2005, **191,** p 375-383
18. C.-J. Li, A. Ohmori, and Y. Harada, Experimental Investigation of the Morphologies of Plasma Sprayed Copper Splats, *Thermal Spraying: Current Status and Future Trends,* A. Ohmori, Ed., May 22–26, 1995 (Kobe, Japan), High Temperature Society of Japan, 1995, p 333-339
19. C.-J. Li and J.-L. Li, Transient Contact Pressure During Flattening of Thermal Spray Doplet and Its Effect on Splat Formation, *J. Thermal Spray Technol.,* 2004, **13**(2), p 229-238
20. R. Kubo, S. Nagakura, A. Inoguchi, and H. Ezawa, Ed., *Physicochemistry Handbook,* Iwanami Shoten Co. Ltd, Tokyo, 1988, p 595.
21. L. Bianchi, A.C. Leger, M. Vardelle, A. Vardelle, and P. Fauchais, Splat Formation and Cooling of Plasma-Sprayed Zirconia, *Thin Solid Films,* 1997, **305,** p 35-47